JANUARY 1976 MATT-1199
Conf.-751125--119

MHD EQUILIBRIUM PROPERTIES OF TOKAMAK FUSION REACTOR DESIGNS

BY

A. M. M. TODD, S. L. GRALNICK,
AND H. E. DALHED

PLASMA PHYSICS LABORATORY

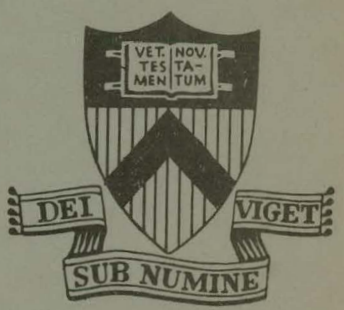

PRINCETON UNIVERSITY
PRINCETON, NEW JERSEY

This work was supported by U. S. Energy Research and Development Administration Contract E(11-1)-3073. Reproduction, translation, publication, use and disposal, in whole or in part, by or for the United States Government is permitted.

DISCLAIMER

NOTICE

Printed in the United States of America.

Available from
National Technical Information Service
U. S. Department of Commerce
5285 Port Royal Road
Springfield, Virginia 22151
Price: Printed Copy $ *; Microfiche $1.45

*Pages	NTIS Selling Price
1-50	$ 4.00
51-150	5.45
151-325	7.60
326-500	10.60
501-1000	13.60

MHD EQUILIBRIUM PROPERTIES OF TOKAMAK FUSION REACTOR DESIGNS*

A. M. M. Todd and S. L. Gralnick
Princeton Plasma Physics Laboratory
Princeton, New Jersey 08540

H. E. Dalhed
University of Wisconsin
Madison, Wisconsin 53706

ABSTRACT

The equilibrium properties of several Tokamak Reactor Designs are analyzed and compared for varying pressure and current profiles using the Princeton Equilibrium Code. It is found that the UWMAK configuration has a broader range of equilibria than the Princeton Reference Design configuration, but that the safety factor on axis is less than unity for peaked current distributions. The Argonne Experimental Power Reactor has a satisfactory range of equilibria, but a means of limiting or diverting the plasma has not yet been proposed, and this may substantially change the results obtained.

---

*Presented at the Sixth Symposium on Engineering Problems of Fusion Research, 18-21 November 1975, San Diego, California.

We describe a study of the MHD equilibrium properties of several proposed Fusion Reactor Designs, namely the Princeton Reference Design (PRD)[1], UWMAK1[2] and UWMAK2[3]. In addition we have investigated equilibria for the Argonne Experimental Power Reactor[4] (EPR). This research was generated by our initial inability to find an equilibrium configuration for the PRD. In the course of understanding this difficulty we were led to investigate the equilibrium properties of the other designs listed above.

The vehicle used in this study was the Princeton Equilibrium Code[5]. This code solves

$$\underline{\nabla} p = \underline{J} \times \underline{B} \tag{1}$$

in the plasma and surrounding vacuum, subject to boundary conditions generated by external coils. Defining the poloidal magnetic flux Ψ in the usual manner,

$$\Psi = \frac{1}{2\pi} \int \underline{B} \cdot \underline{\nabla} \theta \, d\tau \quad , \tag{2}$$

and substituting in (1), we obtain the well known MHD equilibrium equation for the plasma and vacuum,

$$\Delta^* \Psi = \frac{\partial^2 \Psi}{\partial X^2} - \frac{1}{X} \frac{\partial \Psi}{\partial X} + \frac{\partial^2 \Psi}{\partial Z^2} = -4\pi^2 \left(X^2 \frac{dp}{d\Psi} + R^2 g \frac{dg}{d\Psi} \right)$$

$$= -2\pi X J_\phi \quad . \tag{3}$$

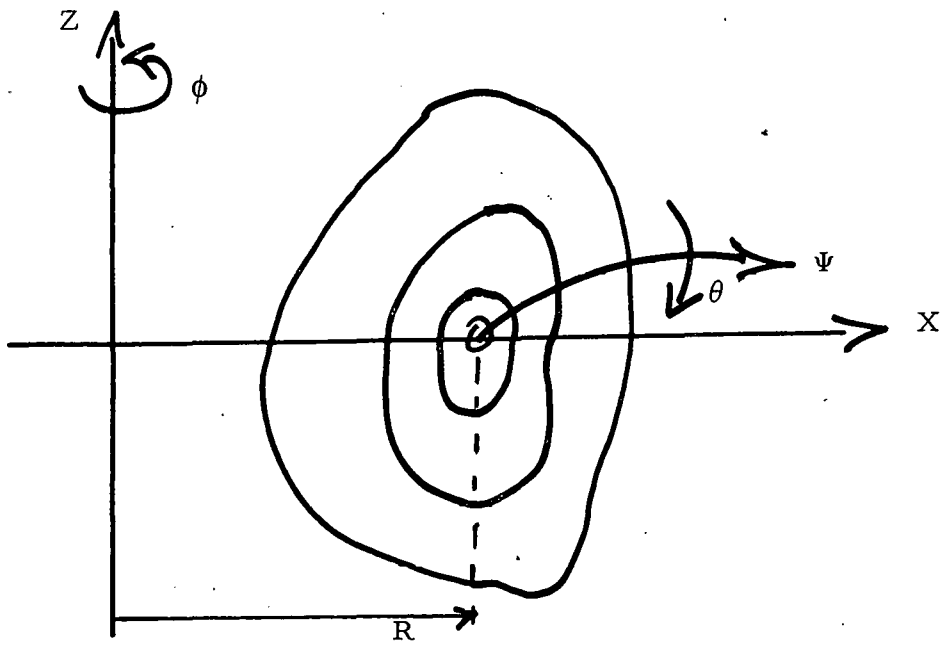

Fig. 1. Coordinate System.

The poloidal magnetic flux is solved as a function of X and Z (see Fig. 1) for prescribed pressure and toroidal field function profiles,

$$p(\Psi) = (p_m - p_\ell)\left(\frac{\Psi_\ell - \Psi}{\Psi_\ell - \Psi_m}\right)^\alpha + p_\ell \quad , \tag{4}$$

and

$$g(\Psi) = XB_\phi = 1 - g_m\left(\frac{\Psi_\ell - \Psi}{\Psi_\ell - \Psi_m}\right)^\beta \quad ,$$

where the subscript ℓ denotes values at the limiting plasma surface - limiter or separatrix - and m denotes values at the magnetic axis. The boundary flux on an arbitrary region of space is obtained as a Green's function solution of the

external coil and plasma currents, where we iterate on (3) until the internal and boundary fluxes have converged. The actual Green's function procedure is that described by von Hagenow[6].

To obtain a solution for a particular design case, we must specify the vacuum toroidal field, the external coil and plasma currents, the pressure at the magnetic axis, and the exponents α and β in equations (4): g_m is calculated to match the given plasma current. $\alpha, \beta = 1$ gives an unrealistic current profile that is almost proportional to the major radius. This can be seen in Fig. 2 which shows an equilibrium solution for UWMAK1 with associated current and pressure profiles, and the local interchange stability properties[7] - the toroidal axis in this and subsequent Figures is on the left. As we increase α and β, the toroidal current becomes increasingly peaked about the magnetic axis (Figs. 3,4,5), with $\alpha, \beta = \infty$ corresponding to the line current solution which was the basis for three of the designs considered; UWMAK2 being the exception. $\alpha=\beta=2$ corresponds approximately to a parabolic current distribution and thus realistic values of α and β would seem to lie in the region of 1.5 to 2.0. The Argonne EPR serics (Fig. 5) has the limiters used in the calculation superimposed on the contours of poloidal magnetic flux. These are not limiters given in the original design, but were added to define the plasma boundary for the code. In

Fig. 4, the PRD wall is superimposed on the contours of flux and is the line that cuts the flux surfaces.

Solutions for the PRD were obtained with a slight modification of the vertical field in the region of the separatrix X-point, and are shown in Fig. 6 for various values of α, β and the vacuum vertical field. A vertical field ratio of one is the given design point. If the vertical field is too strong, the plasma is driven to the inner wall; and if it is too weak, the plasma will drift out and find an equilibrium against the outer wall. In between, there is an acceptable region where the plasma limits on the separatrix, or in the case of the Argonne EPR, on a horizontal limiter rail at the specified minor radius of 2.1 m. This method of limiting the plasma corresponds to an ideal gas blanket. Solutions for the PRD do not exist for $\alpha,\beta > 1.5$, and below that, the sensitivity to changes in the vertical field is too great to make the design acceptable without some revisions. By way of contrast, UWMAK1 and UWMAK2 are very insensitive to changes in the vertical field for all values of α,β as shown in Figs. 7 and 8, but are limited by the safety factor q, defined as

$$q = \frac{1}{2\pi} \frac{\partial}{\partial \Psi} \int \underline{B} \cdot \underline{\nabla} \phi \, d\tau \qquad (5)$$

in the vicinity of the magnetic axis. As the plasma current peaks on axis, that is as α and β increase, the safety

factor decreases until it passes through unity on axis with a resultant local loss of MHD stability. The Argonne EPR has a smaller range in α,β as shown in Fig. 9 but can actually withstand more peaked current distributions than the UWMAKs up to $\alpha,\beta = 2$, before the safety factor on axis reaches unity. A comparison of the four designs without q limits is shown in Fig. 10.

For each of the designs considered, the plasma pressure at the magnetic axis was held constant as we varied α, β and the vertical field. Consequently, as α increases, the volume averaged pressure decreases as the pressure profile peaks on axis. Since the total plasma current is maintained constant, it follows that the average poloidal beta is decreasing as α increases, where the poloidal beta is defined as the volume averaged plasma pressure over the average polodial field pressure at the outer plasma boundary,

$$\beta_\theta = \frac{\int p d\tau / \int d\tau}{\oint_{\Psi_\ell} B_\theta^2 \, dS / \oint_{\Psi_\ell} dS} = \bar{p} < B_\theta^2 >_\ell^{-1} \quad . \qquad (6)$$

In terms of a reactor design where we want beta poloidal as large as possible, this is a more useful parameter for normalizing our results than the pressure on axis. When we do this, we find the previous results are optimistic for two reasons. Firstly, to increase beta poloidal for a given α, we have to increase the pressure at the magnetic axis. This

reduces the equilibrium window above $\alpha, \beta = 1$ by reducing the spread in vertical field for acceptable solutions. A second consequence of increasing the axis pressure is that the current profile is further peaked, driving $q < 1$ at even lower values of α, β, again reducing the equilibrium window. This is demonstrated in Fig. 11 which shows the sensitivity of UWMAK2 at constant beta poloidal, as opposed to Fig. 7 which is for constant pressure at the magnetic axis. It can be seen that the most significant change is the further restriction on the profiles imposed by the q limit, due to the more highly peaked current profiles. Two further points that are not illustrated here, are that increasing the pressure on axis eventually drives reversed currents in the plasma, and also alters the interchange stability properties of the equilibria. However, within their respective equilibrium regions, all the designs were interchange stable.

In order to explain the small band of separatrix limited solutions for the PRD, we generated the teardrop plasma shape with a large current coil on the midplane near the axis of the machine (PRDX). Fig. 10 shows that this resulted in a much broader range of acceptable solutions, suggesting that the problem is not the teardrop plasma shape, but rather the "freedom of motion" of the separatrix surface and x-point. No effort was made to optimize the relative strengths of the coil currents which accounts for the slightly different behavior in this case. The

noncentered solutions are small nonphysical equilibria jammed up against the divertor coil. In the PRD the separatrix surface moves as the plasma moves, whereas in the UWMAKs, the large current divertor coils fix the location of the x-point in their vicinity. The destruction of the PRD magnetic topology is shown in Fig. 13, which is a series of flux plots generated by a line current plasma, where the center figure is the design point. The horizontal series shows the effect on the separatrix surface of moving the magnetic axis in the midplane from outside the design point (left) to inside, and the vertical series shows the effect of changing the vertical field from weaker than design (top) to stronger. If the vertical field necessary for equilibrium at the desired major radius is too weak, the single x-point can separate and become a line near the toroidal axis. Also if the plasma drifts out, the separatrix can break and reform in a figure eight around the vertical field coils. In both cases, the confining magnetic topology is totally disrupted. It should be noted that the x-point moves almost as far as the magnetic axis, so that with this freedom, the separatrix surface readily runs into a wall. In attempting to find equilibrium solutions one both moves the plasma and varies the vertical field at the same time, which in the case of the PRD can easily disrupt the magnetic topology. By way of contrast Fig. 14 shows the same series for the teardrop plasma driven by the large

divertor coil. In this case, the separatrix always closes around the plasma, usually inside the wall, and the x-point hardly moves.

In conclusion, the UWMAK configuration seems to offer the best hope for a reactor design, provided that the safety factor at the magnetic axis can be increased. The elongated UWMAK3 should help alleviate this problem. The PRD plasma configuration would seem to require some redesign with perhaps a feedback system, before satisfactory equilibria can be obtained. It is stressed that the configuration with the large coil on the midplane is not a design suggestion; but rather, was a means of isolating the problems of the original design configuration. The Argonne EPR which was designed without a divertor, seems to have a sufficiently wide range of equilibria, but the problem of limiting or diverting the plasma has not yet been addressed, and as this and other studies have shown, the limiting plasma surface plays a critical role in determining the equilibrium properties.

ACKNOWLEDGEMENT

This work was supported by the United States Energy Research and Development Administration Contract E(11-1)-3073.

REFERENCES

[1]A Fusion Power Plant, R. G. Mills, ed., Princeton Plasma Physics Laboratory Report MATT-1050 (1974).

[2]B. Badger et.al., Wisconsin Toroidal Fusion Reactor Design, University of Wisconsin Report UWFDM-68 (1973).

[3]B. Badger et.al., Wisconsin Toroidal Fusion Reactor Design, University of Wisconsin Report UWFDM-112 (1975).

[4]W. M. Stacey, Jr. et.al., Tokamak Experimental Power Reactor Studies, Argonne National Laboratory Report ANL/CTR-75-2 (1975).

[5]M. S. Chance et.al., Fifth International Conference on Plasma Physics and Controlled Nuclear Fusion Research, (International Atomic Energy Agency, Vienna, 1975) Vol. I, pp. 463-472.

[6]K. v. Hagenow and K. Lackner, Proceedings of the Seventh Conference on the Numerical Simulation of Plasmas, New York (1975).

[7]A. H. Glasser, J. M. Greene, and J. L. Johnson, Phys. Fluids 18, 875 (1975).

PERSPECTIVE VIEW OF POLOIDAL FLUX

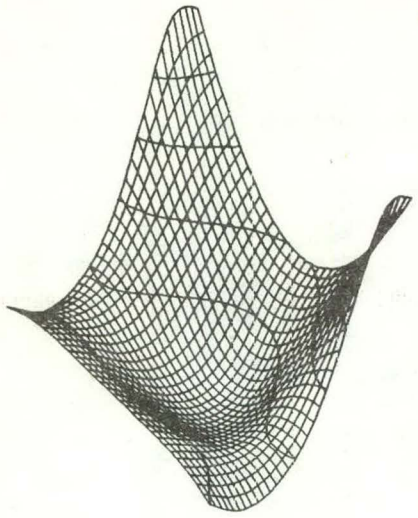

PERSPECTIVE VIEW OF PRESSURE

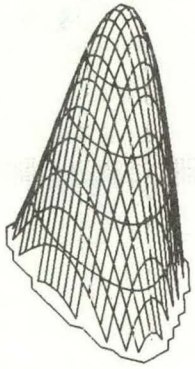

CONTOURS OF POLOIDAL FLUX

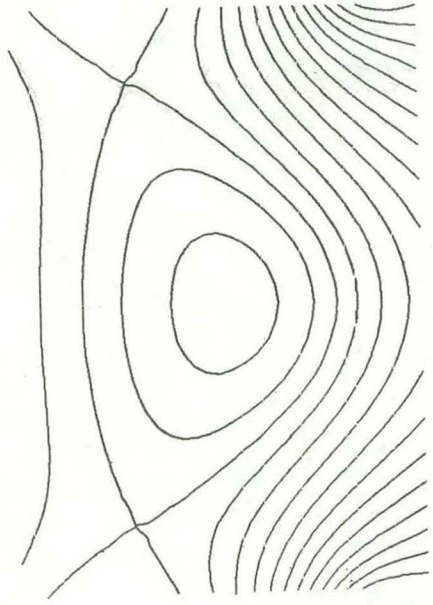

PERSPECTIVE VIEW OF CURRENT

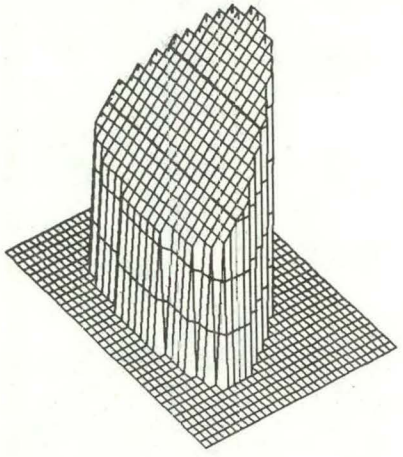

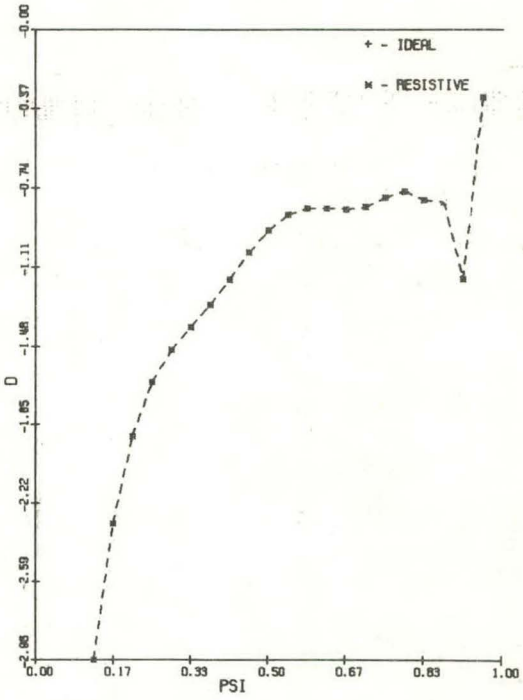

INTERCHANGE STABILITY - D < 0

754602

Fig. 2. UWMAK1 Equilibrium - $\alpha, \beta = 1.$; I = 21 MA.

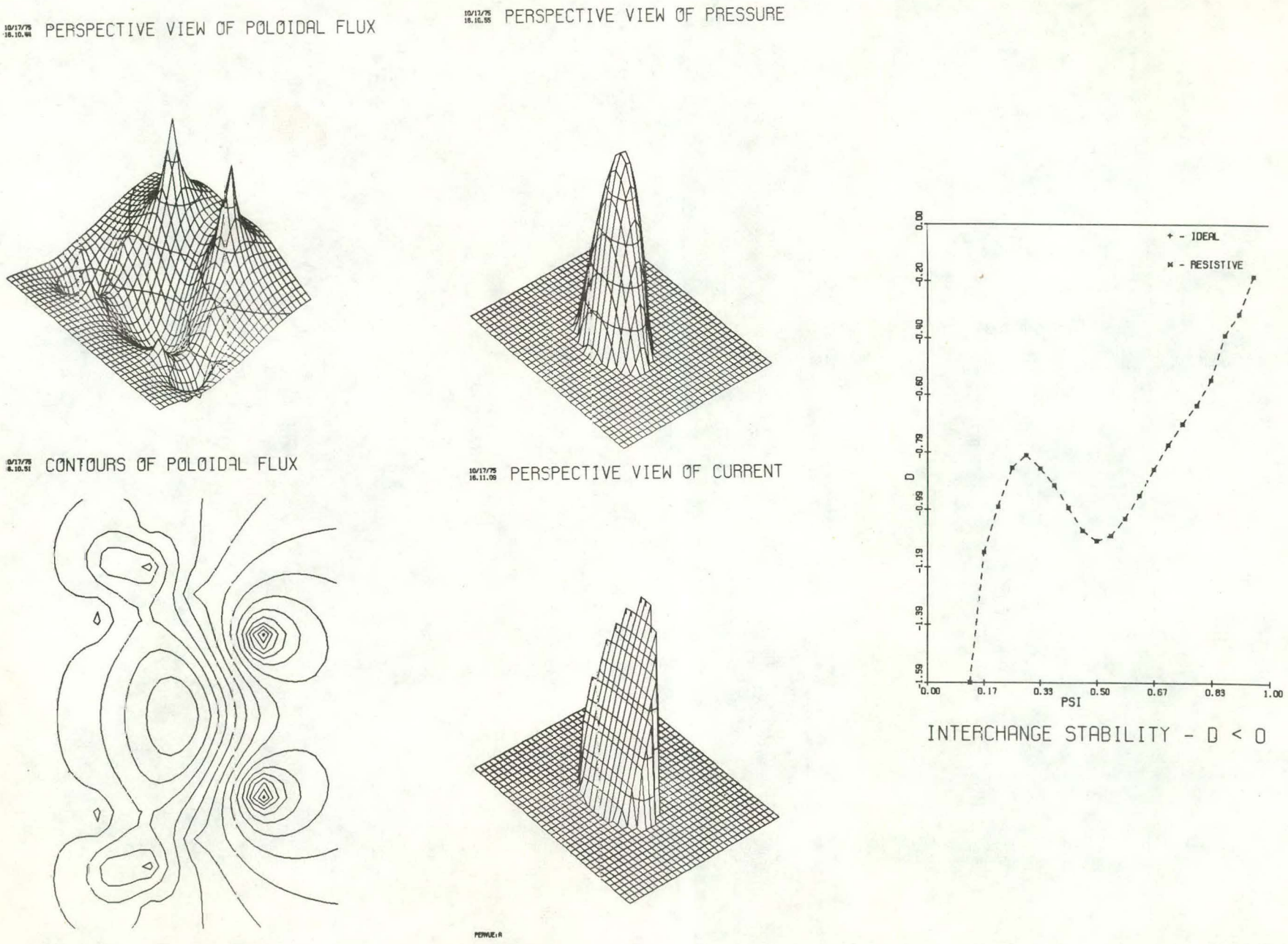

754601

Fig. 3. UWMAK2 Equilibrium - $\alpha, \beta = 1.$; I = 14.9 MA.

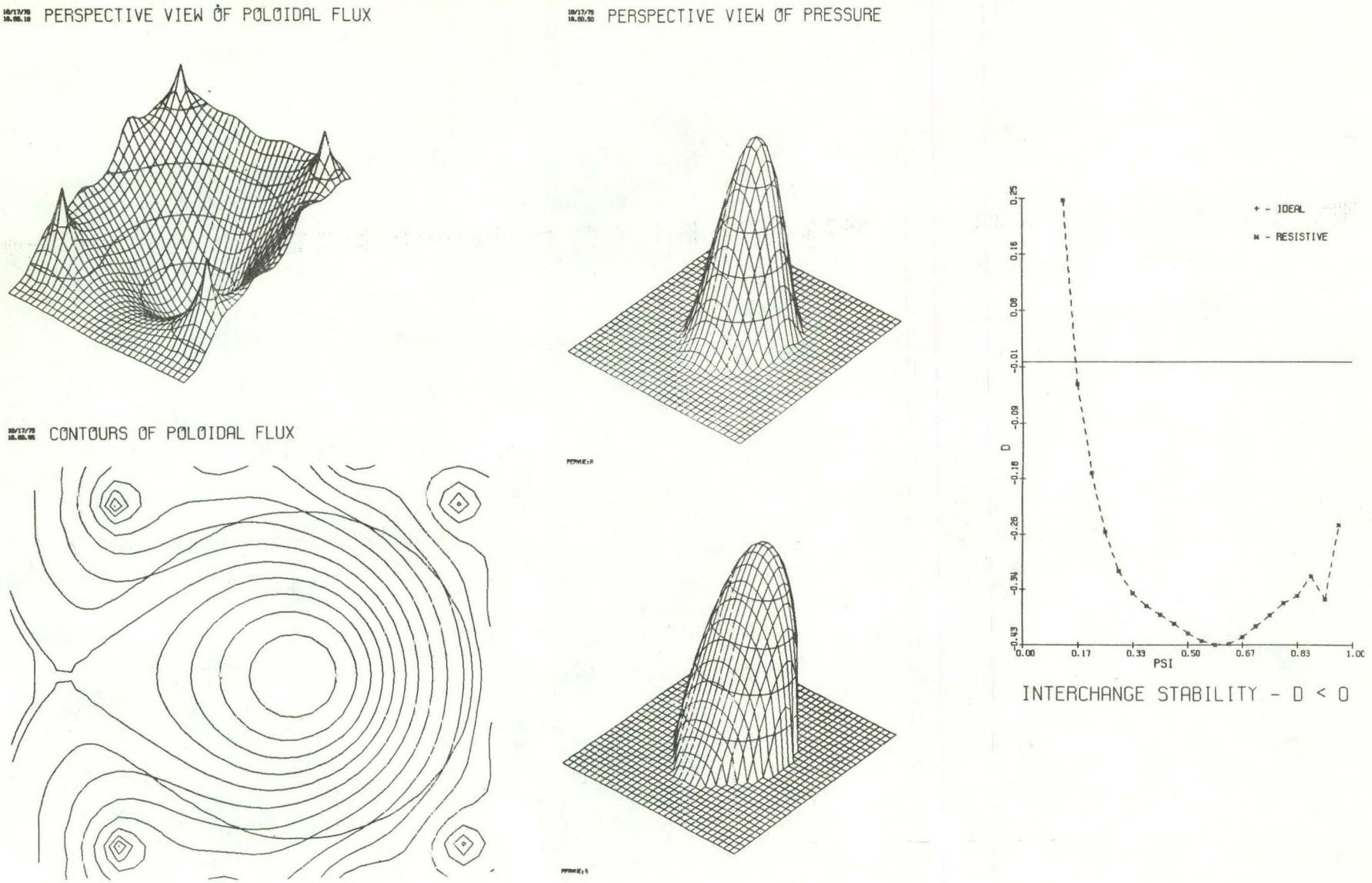

754603

Fig. 4. PRD Equilibrium - $\alpha, \beta = 1.4$; I = 14.6 MA.

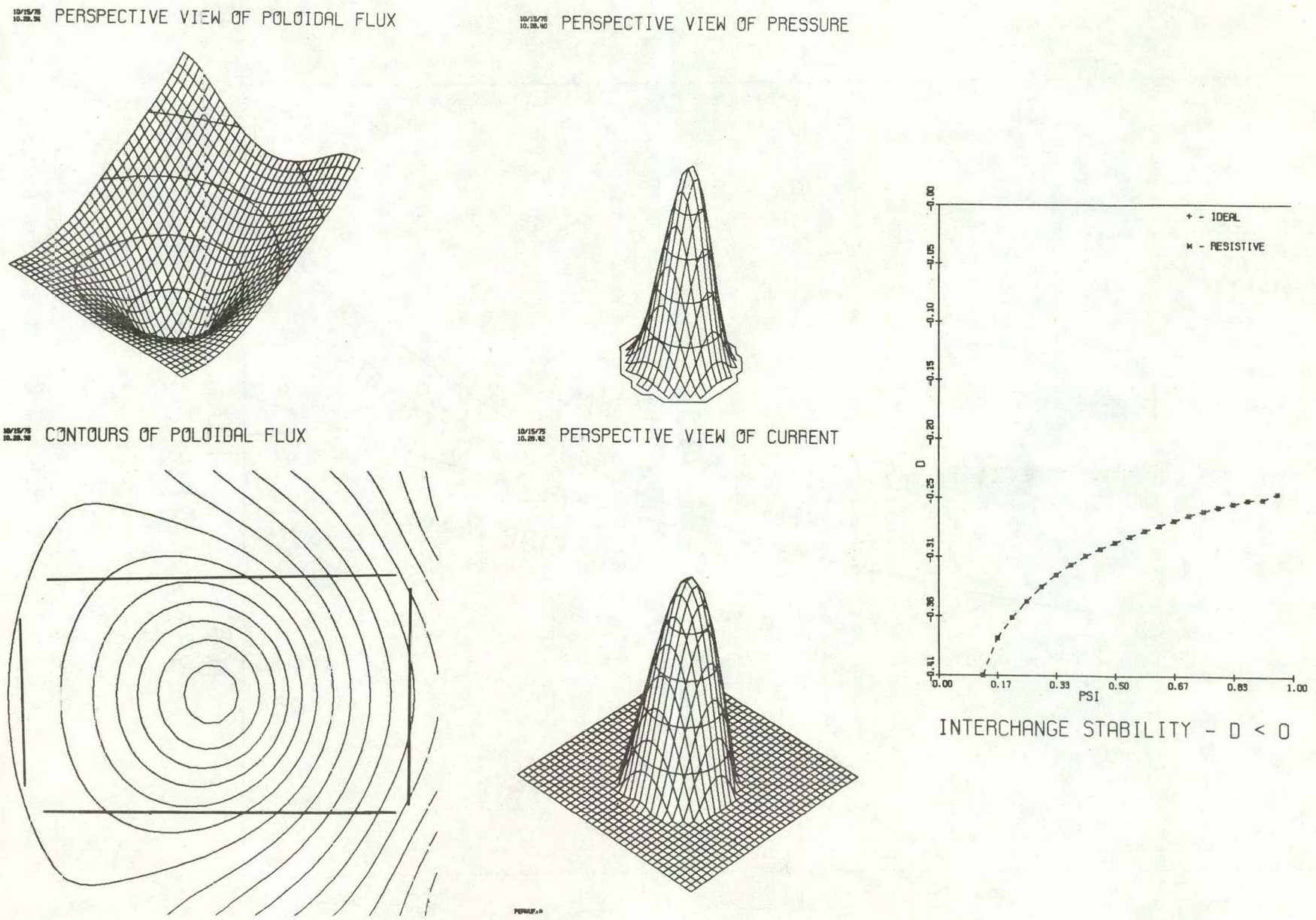

Fig. 5. ANL-EPR Equilibrium - $\alpha, \beta = 2.$; $I = 4.8$ MA.

754604

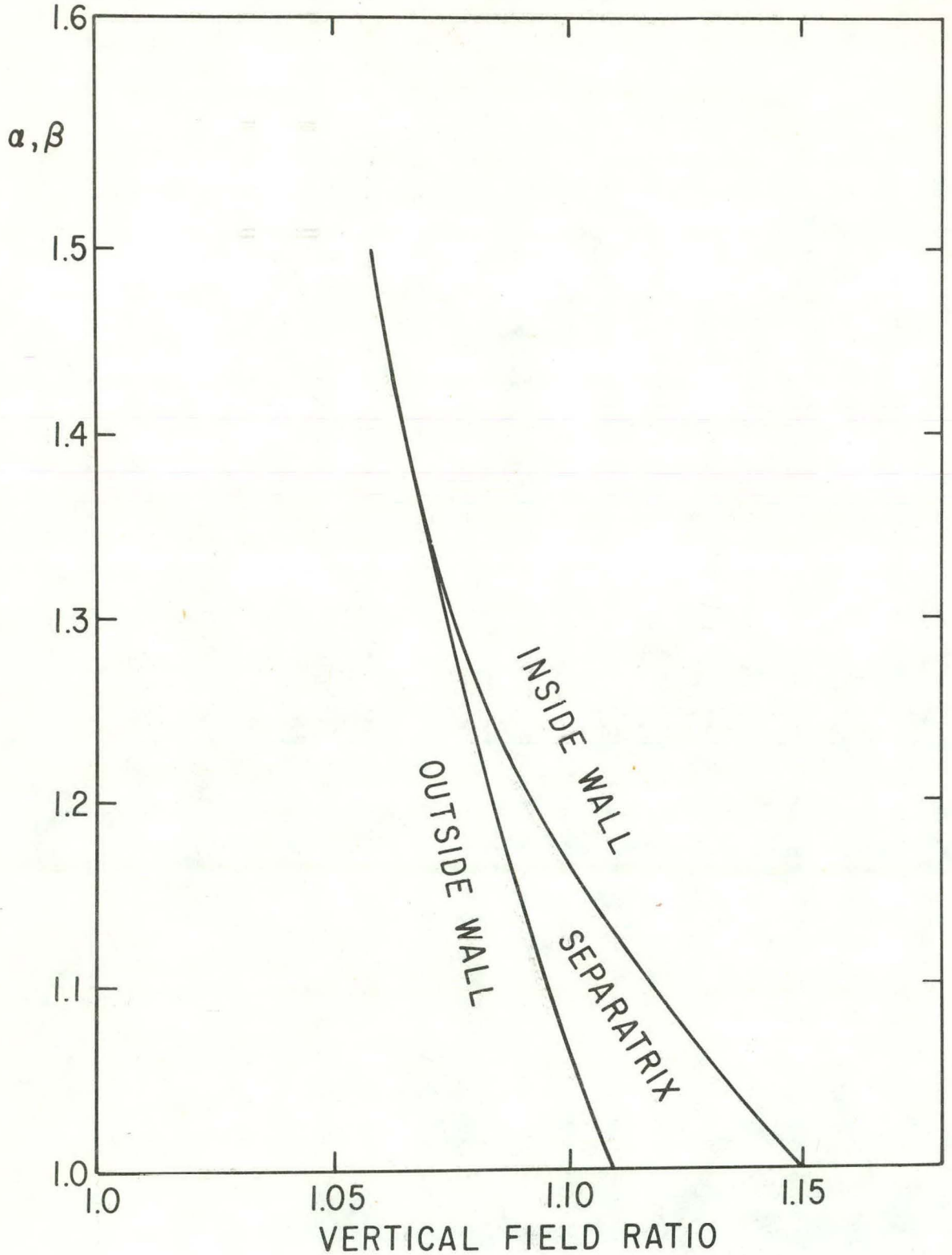

754613

Fig. 6. Plasma Profile Sensitivity of PRD.

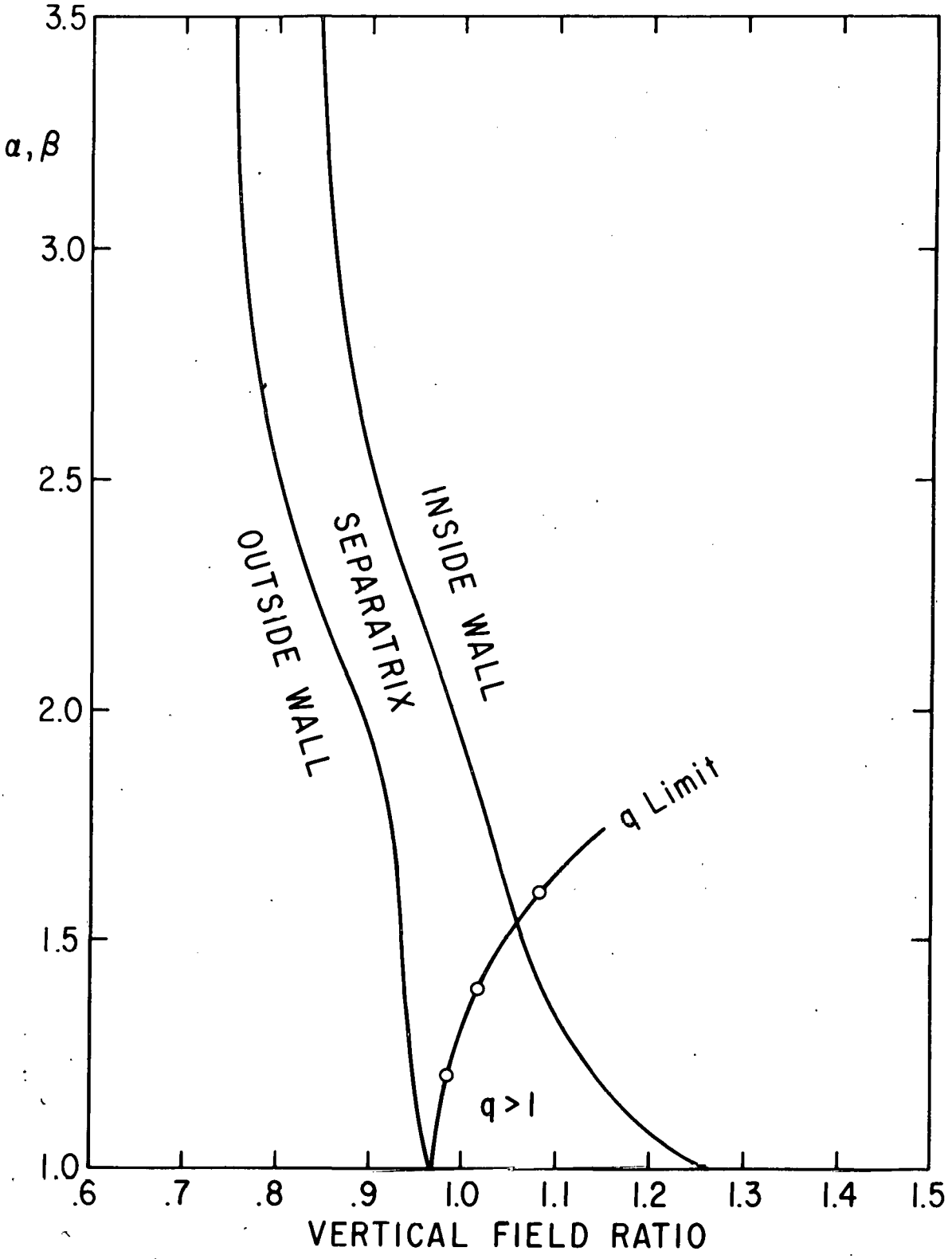

Fig. 7. Plasma Profile Sensitivity of UWMAK2.

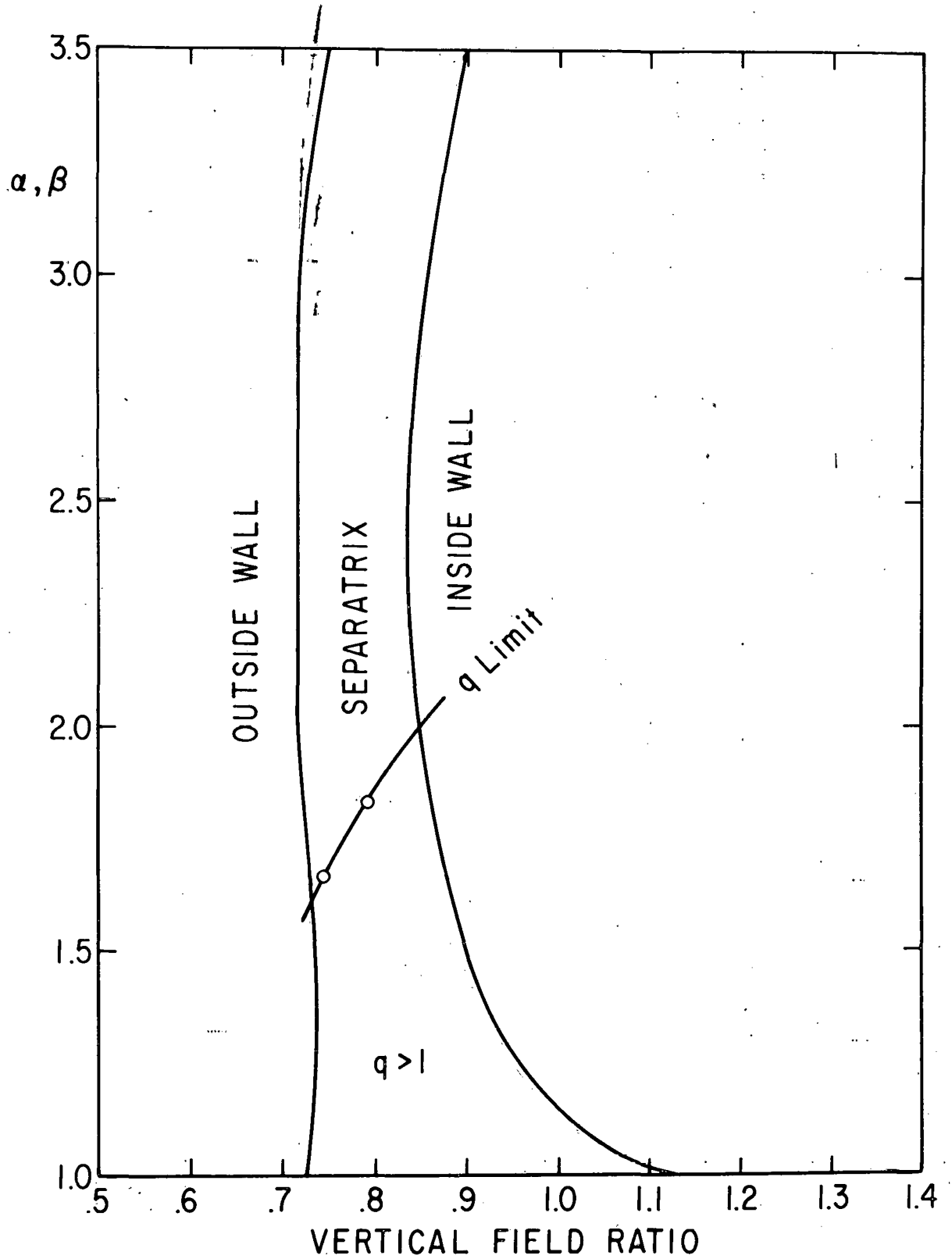

754610

Fig. 8. Plasma Profile Sensitivity of UWMAK1.

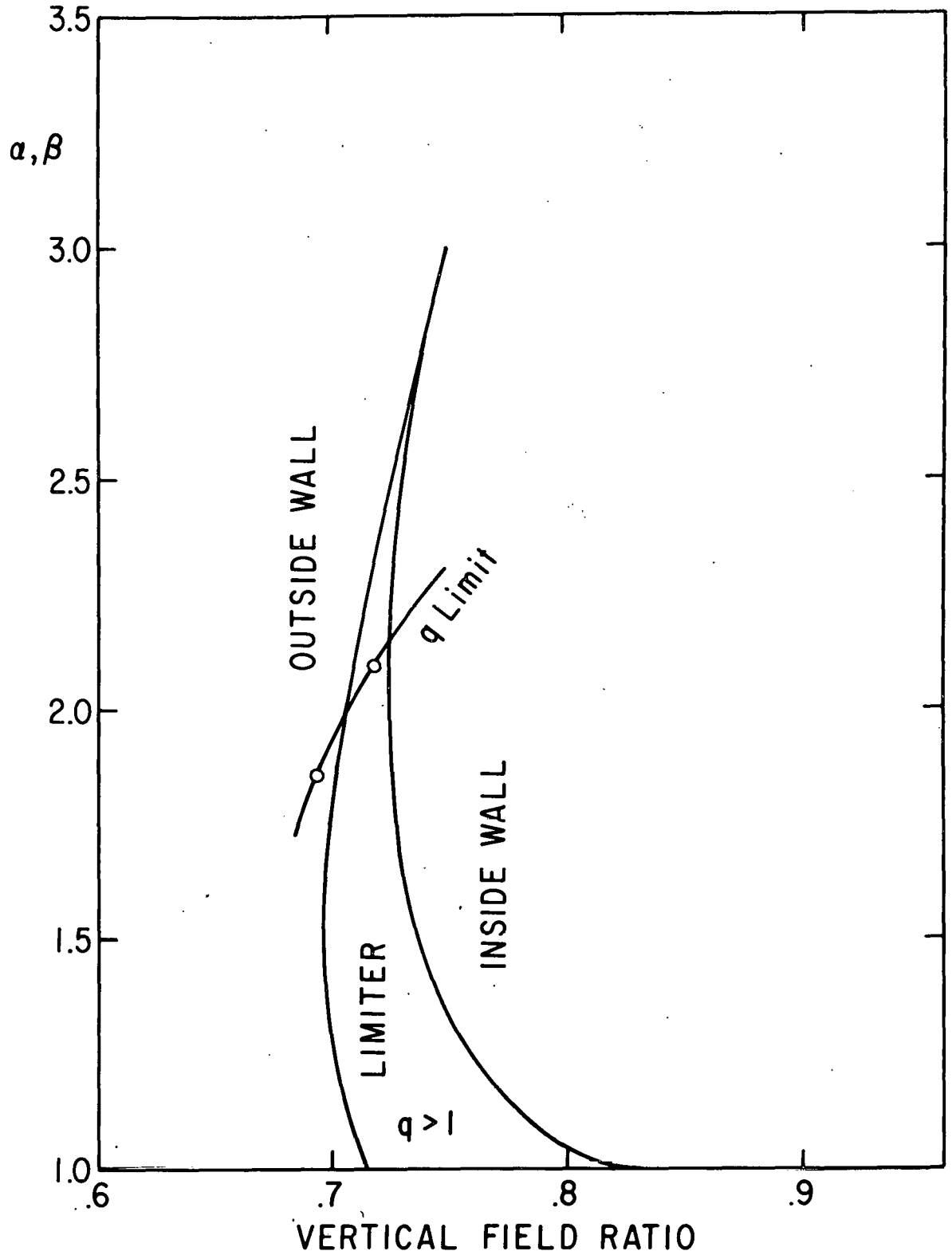

754611

Fig. 9. Plasma Profile Sensitivity of ANL-EPR.

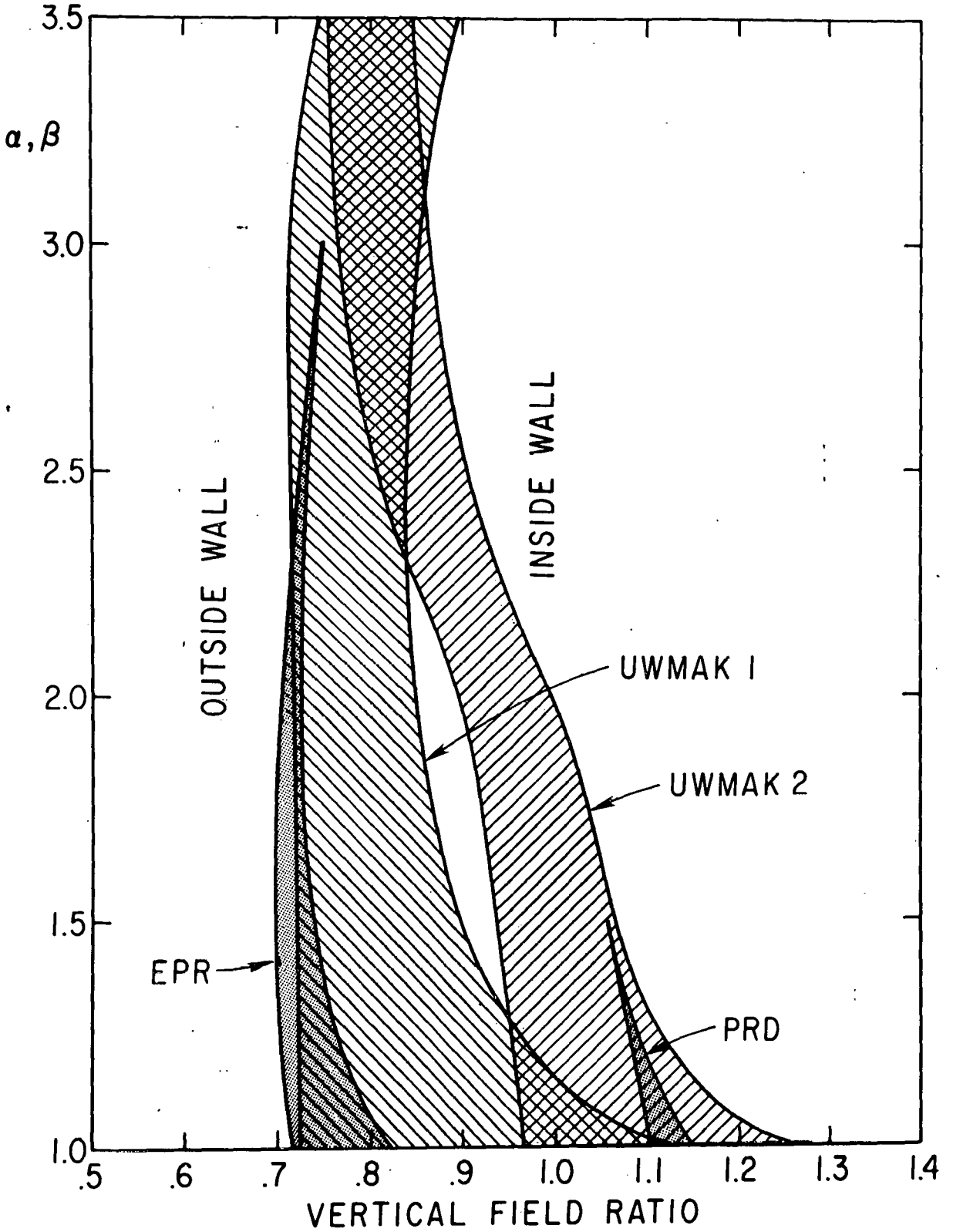

754615

Fig. 10. Plasma Profile Sensitivity of Reactor Designs.

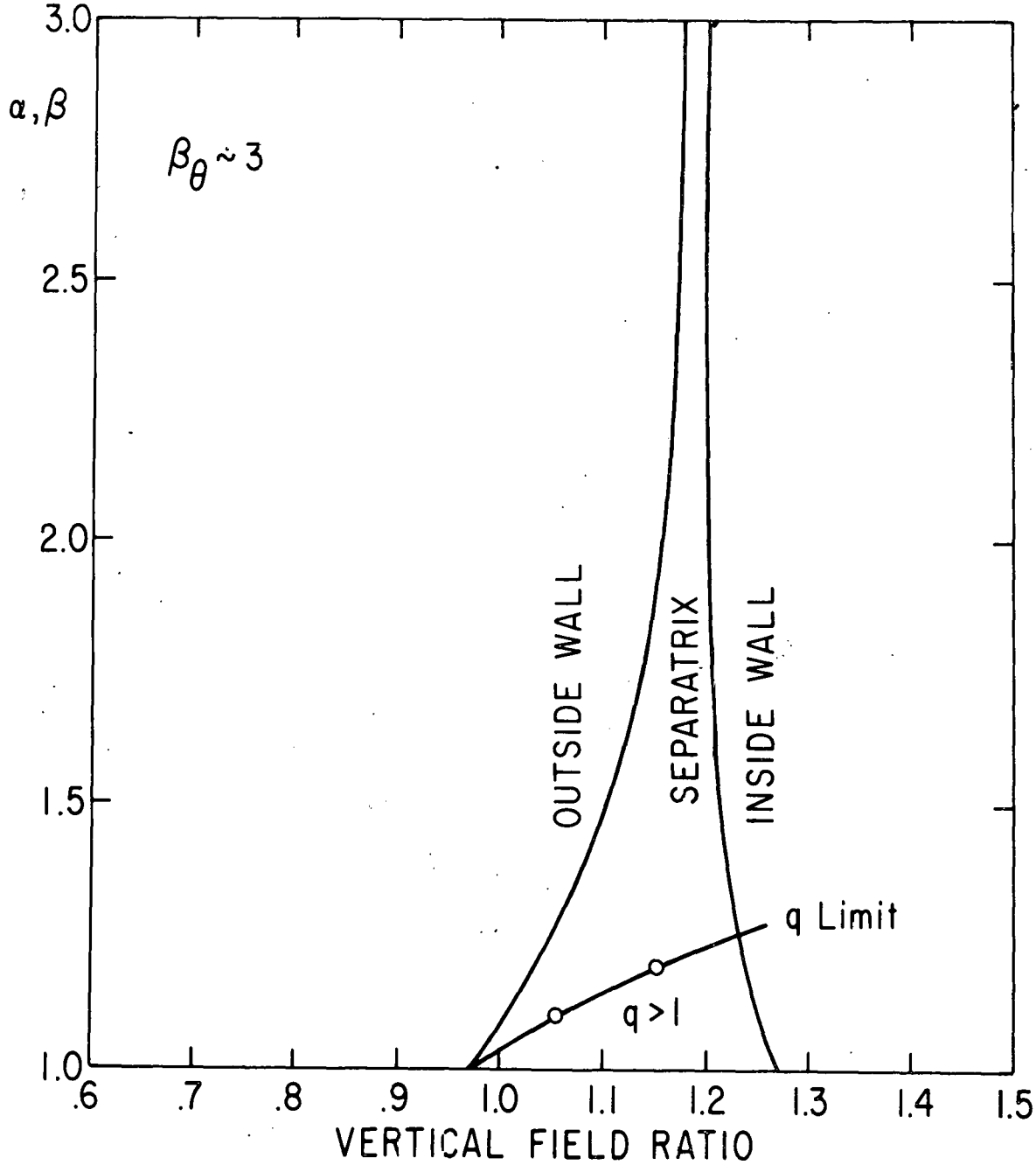

754926

Fig. 11. Plasma Profile Sensitivity of UWMAK2 at constant β_θ.

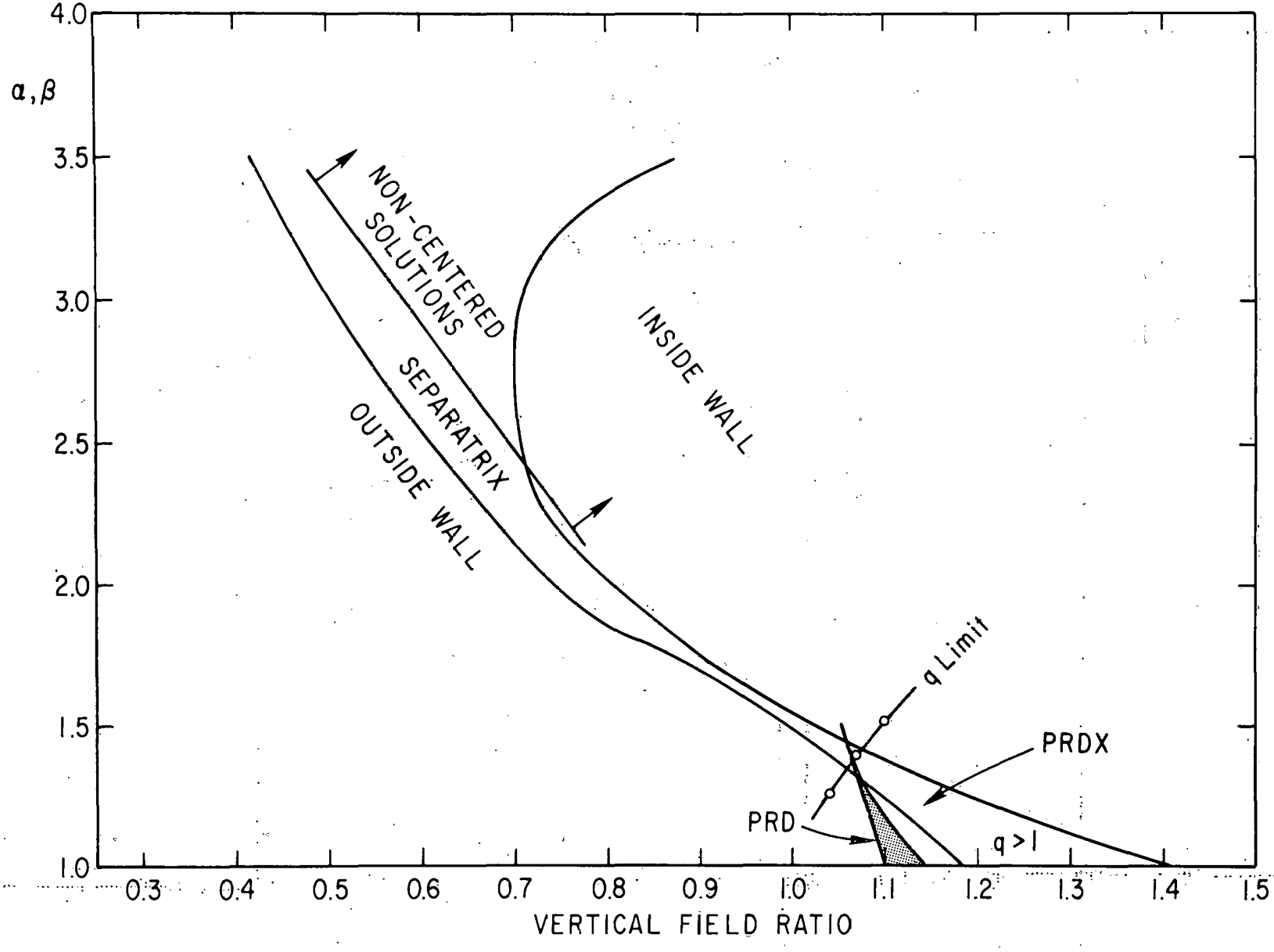

754614

Fig. 12. Plasma Profile Sensitivity of PRDX.

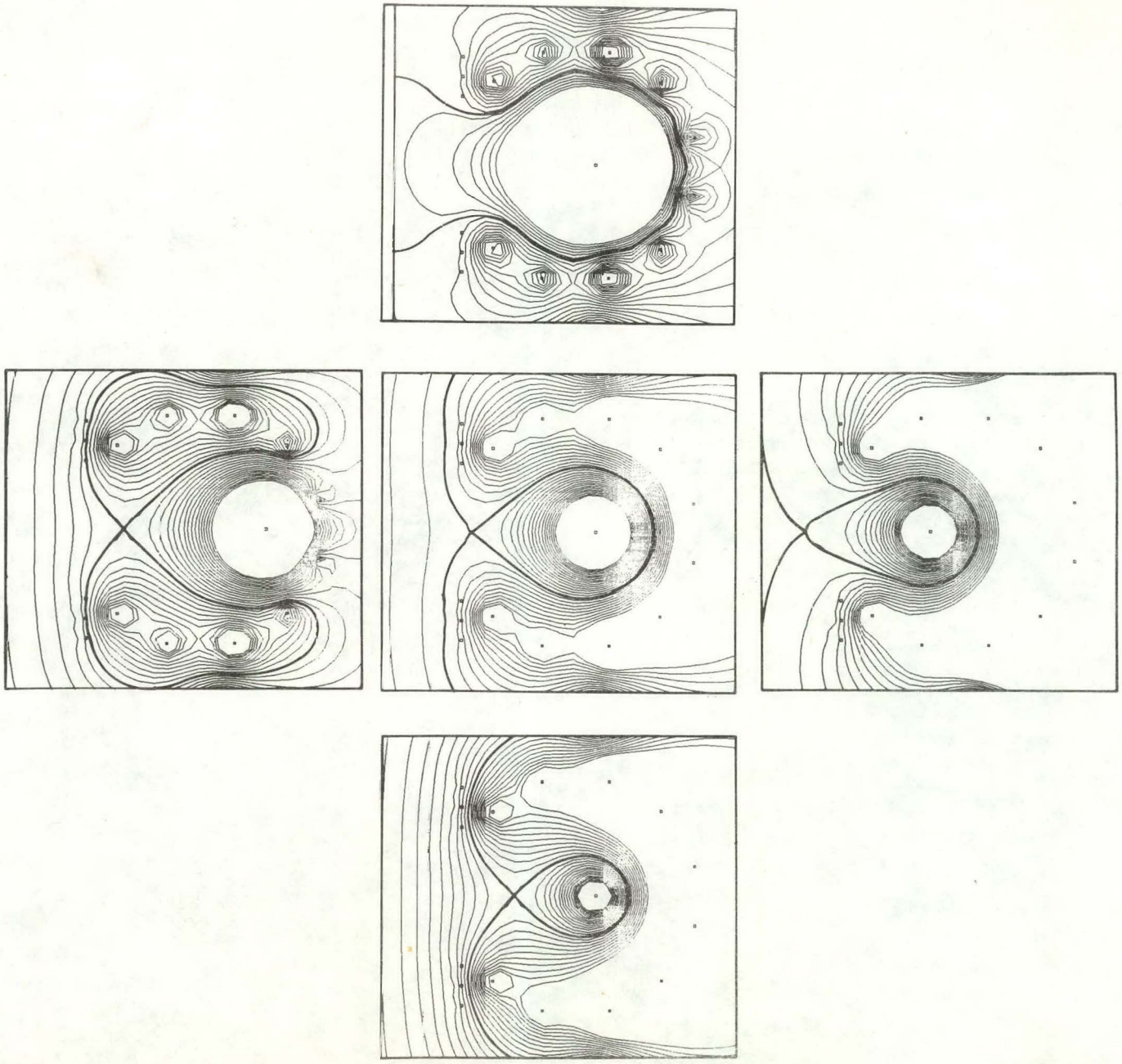

754599

Fig. 13. Magnetic Topology of PRD.

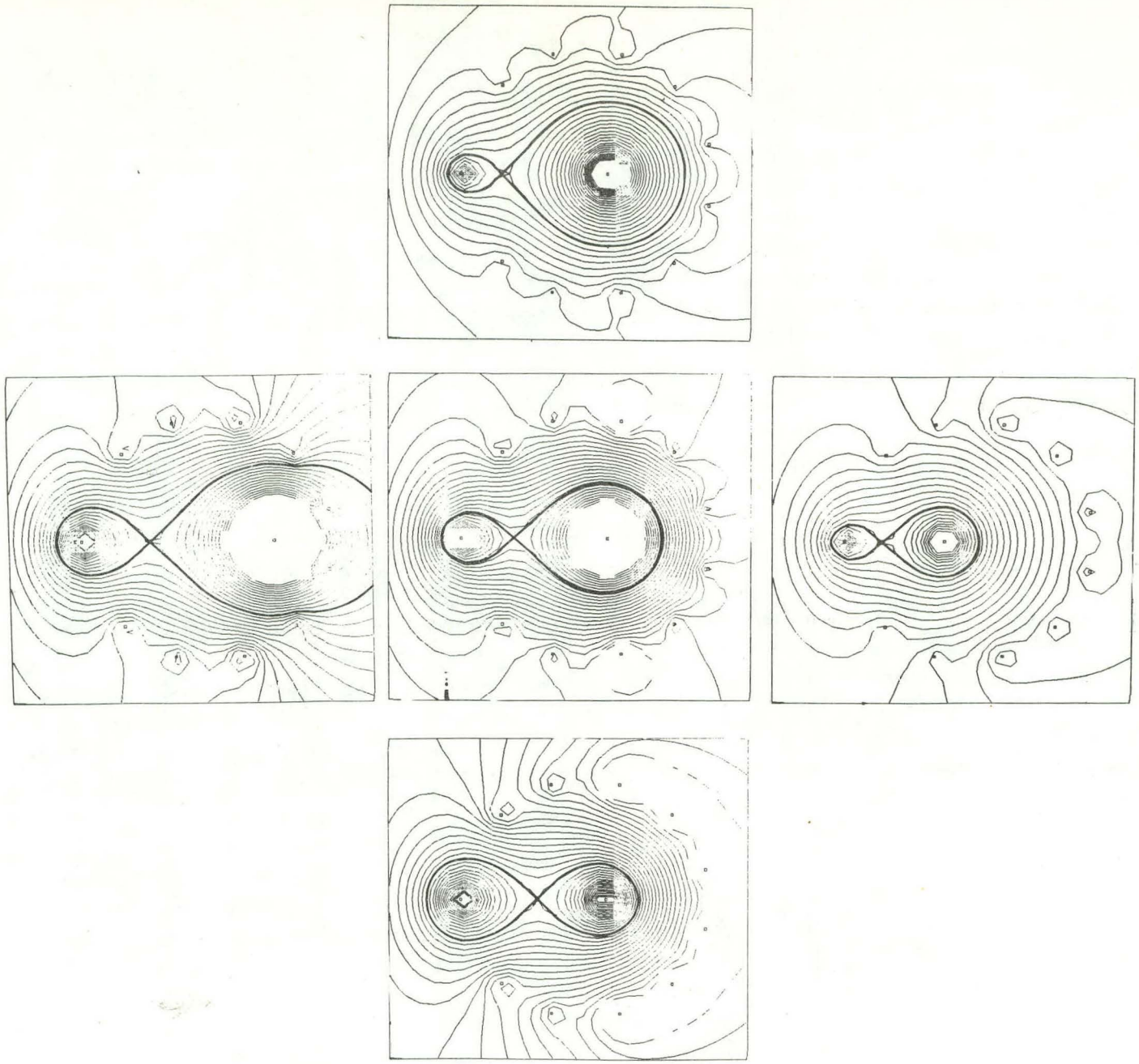

754605

Fig. 14. Magnetic Topology of PRDX.